CHALMERS
UNIVERSITY OF TECHNOLOGY

Integrated Access and Backhaul in Cell-free Massive MIMO Systems

Citation for the original published paper (version of record):
Jazi, A., Mohammad Razavizadeh, S., Svensson, T. (2023). Integrated Access and Backhaul in Cell-free Massive MIMO Systems. IEEE Access, 11: 71658-71667.
http://dx.doi.org/10.1109/ACCESS.2023.3294362

(article starts on next page)

IEEE Access
Multidisciplinary | Rapid Review | Open Access Journal

Received 4 June 2023, accepted 26 June 2023, date of publication 11 July 2023, date of current version 19 July 2023.

Digital Object Identifier 10.1109/ACCESS.2023.3294362

RESEARCH ARTICLE

Integrated Access and Backhaul (IAB) in Cell-Free Massive MIMO Systems

ALI HOSSEINALIPOUR JAZI[1], S. MOHAMMAD RAZAVIZADEH[1], (Senior Member, IEEE), AND TOMMY SVENSSON[2], (Senior Member, IEEE)

[1]School of Electrical Engineering, Iran University of Science and Technology, Tehran 1684613114, Iran
[2]Communication Systems Group, Department of Electrical Engineering, Chalmers University of Technology, 412 96 Gothenburg, Sweden

Corresponding authors: Ali Hosseinalipour Jazi (alihosseinalipour@iust.ac.ir), S. Mohammad Razavizadeh (smrazavi@iust.ac.ir), and Tommy Svensson (tommy.svensson@chalmers.se)

ABSTRACT One of the major challenges with cell-free (CF) massive multiple-input multiple-output (MIMO) networks is providing backhaul links for a large number of distributed access points (APs). In general, providing fiber optics backhaul for these APs is not cost-effective and also reduces network scalability. Wireless backhauling is a promising solution that can be integrated with wireless access links to increase spectrum efficiency. In this paper, the application of integrated access and backhaul (IAB) technique in millimeter-wave (mmWave) CF massive MIMO systems is investigated. The access and backhaul links share a frequency spectrum in the mmWave bands, and in both, hybrid beamforming techniques are adopted for signal transmission. The bandwidth allocation (division) parameter between the two link types as well as the beamforming matrices are optimized to maximize the end-to-end data rate. This leads to a non-convex optimization problem for which an efficient solution method is proposed. The simulation results show the effectiveness of the IAB technique and our proposed scheme in CF massive MIMO systems. These simulations also compare the proposed hybrid beamforming method with a fully digital solution in terms of the number of radio frequency (RF) chains and the volume of backhaul traffic. Finally, the effect of increasing the number of APs on the users' data rates in terms of wireless access and backhaul links constraints is also examined.

INDEX TERMS Integrated access and backhaul (IAB), massive MIMO, millimeter-wave (mmWave), cell-free (CF), hybrid beamforming.

I. INTRODUCTION

During past years, there have been increasing demands for new wireless services like enhanced mobile broadband (eMBB) and ultra-reliable and low latency communication (URLLC) that motivate researchers to develop new technologies for efficient and reliable transmission of more data in minimal time and frequency resources. Massive multiple-input multiple-output (MIMO) is one of the promising techniques for accommodating these demands [1]. However, implementation of a large number of antennas of massive MIMO on a limited space base station (BS) is not easy in practice and leads to a degradation in the expected performance. In addition, in the centralized implementation scenarios of the massive MIMO arrays, there is a significant difference in the signal powers of cell-edge and cell-center users. This motivates distributed or cell-free (CF) massive MIMO systems in which the antennas of the massive MIMO are distributed among a number of access points (APs) in a wide area [2]. CF massive MIMO systems can provide uniform quality of service (QoS) over a cell region and reduce multi-user interference [3]. It is also a good choice for implementing new services like massive machine type communication (mMTC) and internet of things (IoT), in which devices are distributed in a wide service area [4].

In the CF networks, a large number of APs are connected to a central processing unit (CPU) via backhaul links. Each AP uses spatial multiplexing techniques to serve all network users simultaneously with the same time-frequency resources. Separating users signals via beamforming can be

The associate editor coordinating the review of this manuscript and approving it for publication was Stefan Schwarz.

achieved by centralized beamforming at the CPU or decentralized beamforming at each AP. In the centralized scenario, all APs need to send their channel state information (CSI) to the CPU over the backhaul link, but in the decentralized scenario, each AP calculates the beamforming matrices based on the local CSI. Therefore, the decentralized beamforming reduces the backhaul link traffic. For example, in [5] authors introduce a distributed hybrid beamforming approach in which APs and CPU jointly optimize the beamforming matrices. The simulation results show that the performance of the proposed hybrid beamforming algorithm is very close to the fully digital beamforming and reaches the performance of the centralized scenario. Another approach to reduce the backhaul link resources and increase CF network scalability is the user-centric (UC) idea where each user is served by a limited number of APs based on their channel conditions. The simulation results in [6] show that UC achieves a higher data rate for each user for the vast majority of users using fewer backhaul resources compared to the traditional CF approach.

CF networks usually face many challenges, including synchronization among the APs, user association, and backhaul link provisioning for the APs [7]. Considering a wired backhaul link is a common assumption during these years as the wireless backhaul link faces the conventional challenges of the wireless environment, including higher interference and lower data rates compared to the wired backhaul link. However, existing cable and optical fiber-based backhaul links are less suitable for future cellular networks due to implementation costs and low flexibility. Hence, the wireless backhaul has attained much attention due to its lower implementation complexity and higher flexibility [8]. Microwave backhaul links that operate in line-of-sight (LOS) conditions have been used for a long time, utilizing dedicated international telecommunications union (ITU) frequency bands [9]. However, in 5G, millimeter-wave (mmWave) frequency bands are a potential candidate to meet the growing bandwidth demand in the future wireless backhaul link. In addition, due to the wide bandwidth in the mmWave access spectrum, there is a new interest to share radio resources between the wireless backhaul and access links, leading to the concept of integrated access and backhaul (IAB) [10].

There are many papers that study wireless backhauling and IAB techniques in wireless cellular networks. For example, in [11], the authors consider a cellular heterogeneous network (HetNet) with wireless backhaul links and design the beamforming matrices for this network. The authors in [12] maximize the wireless backhaul link rate in the mmWave bands and then use this rate as a constraint in maximizing the rate of users in the access link that operate in the sub-6 GHz frequency band. The design of IAB networks by multiplexing the access and backhaul links in time domain is studied in [13]. The authors in [14] maximize end-to-end sum rate of users (i.e., from the CPU in the network core to the users) in a mm-wave cellular network by optimizing the dedicated bandwidth for the access and backhaul links and power allocation coefficients in the macro-cell BS (MBS). In addition, the authors in [9] and [15] evaluate the coverage probability of a cellular network equipped with IAB by considering different backhaul scenarios (fiber, wireless/fiber, and IAB). In the case of wireless backhauling, the small-cell BSs (SBSs) in the backhaul link and users in the access link are served by different carrier frequencies. In most of the references, the authors do not optimize the bandwidth allocation coefficient between the access and backhaul connections and use a frequency division multiplexing in the access and backhaul links [16].

There are also a few papers that assume wireless backhauling in the CF networks. For example, in [17] and [18], the wireless backhaul links parameters are considered as the constraints for the access link optimization in the CF networks. In [19] the authors optimize end-to-end rate in a UC-CF network by jointly optimizing the beamforming matrix in the backhaul link and the power allocation coefficients in the access link. This paper considers different frequency bands (mm-wave band and sub-6 GHz) for the access and backhaul links. However, to the best of our knowledge, the IAB technique and specially frequency multiplexing between backhaul and access links in the CF networks has not been studied before in the literature.

In this paper, we study the use of IAB in the downlink of a CF massive MIMO network in which the wireless backhaul and access links are multiplexed in the frequency domain. In the considered network, there is one CPU (IAB-donor) and multiple APs (IAB-nodes) that serve a large number of users at the same time and frequency resource. In this paper, we use the terms CPU/APs and IAB-donor/IAB-nodes interchangeably. We assume that both wireless access and backhaul links operate in the same mm-wave frequency band, and hybrid beamforming techniques are used for signal transmission at both of them. For optimal design of the IAB scheme, we optimize the bandwidth allocation coefficient between the access and backhaul links to maximize the minimum end-to-end rate over them. At the same time, the hybrid beamforming matrices at the CPU and APs are also optimized, which finally leads to a non-convex optimization problem that cannot be solved efficiently. Hence, we propose a solution method that optimizes the above variables for access and backhaul links alternatively. We also derive a closed-form expression for dividing the mm-wave frequency band between the access and backhaul links. We verify the performance of the proposed scheme through computer simulations. The results show the effectiveness of using IAB in the CF massive MIMO systems. We also evaluate the performance of the proposed hybrid beamforming optimization scheme by comparing it with fully digital beamforming and centralized beamforming at the CPU, which illustrates the effectiveness of using this technique in conjunction with IAB. Then, we investigate the impact of the number of APs on coverage enhancement of the CF network in the access link and also on the rate of the backhaul link. Finally, by considering the effects of both the access and backhaul rates on the end-to-end rate of the networks, we show that in the CF massive MIMO systems

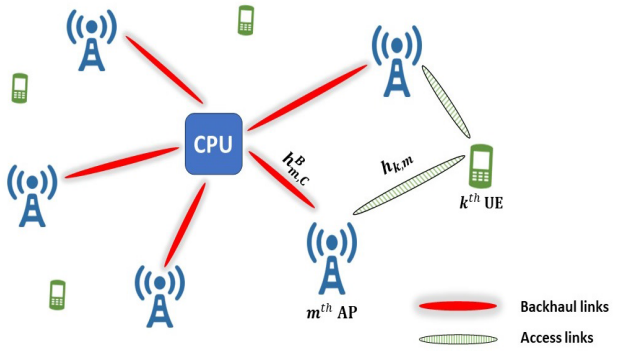

FIGURE 1. System Model of a cell-free Massive MIMO Network with Integrated Access and Backhaul (IAB).

with wireless backhaul, there is an optimal number of APs achieving the best performance.

The rest of this paper is organized as follows. The system model is described in Section II. Following the definition of the main problem in Section III, the parameters of the backhaul and access links are optimized in Sections IV and V, respectively. Section VI specifies a closed-form equation for the bandwidth allocation coefficient. Section VII presents the numerical results of the proposed algorithms. In Section VIII, the paper is summarized.

Throughout this paper, the following notations are used: a, $\mathbf{a}$, and $\mathbf{A}$ stand for a scalar, a column (or row) vector, and a matrix, respectively; $[\mathbf{A}]_{i,j}$ denotes the $(i;j)$-th element of matrix $\mathbf{A}$ and the i-th element of vector $\mathbf{a}$ is denoted by $[\mathbf{a}]_i$; $rank(\mathbf{A})$ is the rank of $\mathbf{A}$; $(\mathbf{A})^*$, $(\mathbf{A})^T$, and $(\mathbf{A})^H$, denote conjugate, transpose, and Hermitian transpose of $\mathbf{A}$, respectively. The Euclidean and Frobenius norms of $\mathbf{A}$ are denoted by $\|.\|$ and $\|.\|_F$, respectively. Furthermore, we use $Tr\{\}$, $\Re\{\}$, and $\mathbb{E}\{\}$ to respectively represent the trace, real part taking, and expectation operators. $diag\{\mathbf{a}\}$ forms a diagonal matrix of the vector $\mathbf{a}$, and $\mathbf{I}_N$ denotes the $N \times N$ identity matrix. $z \sim \mathbb{CN}(0, \sigma^2)$ denotes a circularly symmetric complex Gaussian random variable z with zero mean and variance σ^2. Further, $\mathbb{C}$ and $\mathbb{C}^{m\times n}$ describe a complex value and a complex matrix of dimension $m \times n$, respectively. The amplitude and phase of a complex value z are denoted by $|.|$ and $\angle$, respectively.

II. SYSTEM MODEL

As depicted in Fig. 1, we consider a CF massive MIMO system consisting of M N_A-antenna APs (i.e., IAB-nodes) that serve K single-antenna users. All the IAB-nodes are connected to an N_C-antenna CPU (i.e., IAB-donor). Since the focus of this study is on the integration of the access and backhaul links in CF networks, we assume for simplicity that each AP serves all users and leave the concept of UC-CF to future works. Both the access and backhaul links operate at the same frequency band in the mmWave frequencies. All the access and backhaul links are served by full-duplex APs. We assume that B and $\eta \in (0, 1]$ indicate the total available bandwidth in the network and the bandwidth allocation coefficient between the access and backhaul links, respectively. Thus, the dedicated bandwidth to the access and backhaul links become ηB and $(1-\eta)B$, respectively. In the following, we discuss signal transmission and reception in the access and backhaul links.

A. ACCESS LINK

Let $x_k \in \mathbb{C}$ denotes the k-th user's signal in the access link, which is transmitted from all the APs and $\mathbb{E}\{|x_k|^2\} = 1$. The received signals at the k-th user is

$$\begin{aligned} y_k &= \sum_{m=1}^{M}\sum_{j=1}^{K} \mathbf{h}_{k,m}\mathbf{W}_m^{RF}\mathbf{w}_{j,m}^{BB}x_j + n_k \\ &= \underbrace{\sum_{m=1}^{M} \mathbf{h}_{k,m}\mathbf{W}_m^{RF}\mathbf{w}_{k,m}^{BB}x_k}_{Desired\ signal} + \underbrace{\sum_{m=1}^{M}\sum_{\substack{j=1\\ j\neq k}}^{K} \mathbf{h}_{k,m}\mathbf{W}_m^{RF}\mathbf{w}_{j,m}^{BB}x_j}_{Interference} \\ &\quad + n_k, \end{aligned} \tag{1}$$

where $\mathbf{W}_m = \mathbf{W}_m^{RF}\mathbf{W}_m^{BB} \in \mathbb{C}^{N_A\times K}$ denotes the hybrid beamforming matrix of the m-th AP which is product of an analog beamforming matrix $\mathbf{W}_m^{RF} \in \mathbb{C}^{N_A\times N_{RF}^A}$ and a baseband digital beamforming matrix $\mathbf{W}_m^{BB} \in \mathbb{C}^{N_{RF}^A\times K}$ (where $\mathbf{w}_{k,m}^{BB}$ is the k-th column of $\mathbf{W}_m^{BB}$). Here, N_{RF}^A is the number of RF chains at each AP. The analog beamforming matrix has a unit-module constraint (i.e., $\left|[\mathbf{W}_m^{RF}]_{i,j}\right| = \frac{1}{\sqrt{N_A}}$) and the digital beamforming matrix must satisfy AP power constraint $\|\mathbf{W}_m^{BB}\|_F^2 \leq P^A$, where P^A is the total AP's power constraint for the access link. In addition, $n_k \sim \mathbb{CN}(0, \sigma_k^2)$ is the additive white Gaussian noise at the k-th user.

The channel gain of the m-th AP to the k-th user is denoted by $\mathbf{h}_{k,m} \in \mathbb{C}^{1\times N_A}$ that follows Saleh-Valenzuela (SV) channel model [20], [21] and is defined as

$$\begin{aligned} \mathbf{h}_{k,m} &= \sqrt{N_A}\,\vartheta_{k,m}^{L}\,\mathbf{a}_L(\varphi_{k,m}^{AoD}) \\ &\quad + \sum_{l=1}^{L_{k,m}} \sqrt{\frac{N_A}{L_{k,m}}}\,\vartheta_{l,k,m}^{N}\,\mathbf{a}_L(\varphi_{l,k,m}^{AoD}). \end{aligned} \tag{2}$$

In this equation, $L_{k,m}$, $\varphi_{k,m}^{AoD}(\varphi_{l,k,m}^{AoD})$, and $\mathbf{a}_L(.)$ represent the number of non-line-of-sight (NLOS) paths, the angle of departure, and the normalized array response vector, respectively. Without loss of generality, we consider a uniform linear array (ULA) at each AP and CPU. For an N-element ULA, the array response can be expressed as

$$\begin{aligned} \mathbf{a}_L(\varphi) &\triangleq \frac{1}{\sqrt{N}}\left[1,\ e^{j\frac{2\pi}{\lambda}d_A\sin(\varphi)},\ \ldots,\ e^{j\frac{2\pi}{\lambda}d_A(N-1)\sin(\varphi)}\right] \\ &\in \mathbb{C}^{1\times N}, \end{aligned} \tag{3}$$

where λ is the wavelength, and d_A indicates inter-element spacing. Also, $\vartheta_{k,m}^{L} \in \mathbb{CN}\left(0, I(d)\,10^{-0.1\kappa}\right)$ indicates path loss of the channel between the m-th AP and the k-th user in the LOS link, in which $I(d)$ is a parameter that shows the existence of a LOS link between APs and users, where $I(d) = 1$ means there is a LOS link in the access link by

probability ρ, which for Urban Microcellular (UMi) scenario can be defined as [22]

$$\rho = \min\left(\frac{20}{d}, 1\right)\left(1 - e^{\frac{-d}{39}}\right) + e^{\frac{-d}{39}}. \tag{4}$$

Similarly, $\vartheta^N_{l,k,m} \in \mathbb{CN}\left(0, 10^{-0.1\kappa^N}\right)$ determines the NLOS link path loss model. Here, κ is also obtained as below [23]

$$\kappa = 32.4 + 20\log_{10}(f_c) + 10\log_{10}(d^{\alpha}), \tag{5}$$

where f_c, d, and α represent the carrier frequency in GHz, distance between transmitter and receiver in meter, and the channel path loss exponent, respectively.

The signal-to-interference-plus-noise-ratio (SINR) at each user (in the access link) can be expressed as

$$SINR^A_k = \frac{\sum_{m=1}^{M}\left|\mathbf{h}_{k,m}\mathbf{W}^{RF}_m\mathbf{w}^{BB}_{k,m}\right|^2}{\sum_{\substack{j=1\\ j\neq k}}^{K}\sum_{m=1}^{M}\left|\mathbf{h}_{k,m}\mathbf{W}^{RF}_m\mathbf{w}^{BB}_{j,m}\right|^2 + \sigma^2_k}. \tag{6}$$

Thus, the sum rate of all users in the access link becomes

$$R^A = \eta B \sum_{k=1}^{K}\log\left(1 + SINR^A_k\right). \tag{7}$$

B. BACKHAUL LINK

In the backhaul link, the IAB-donor with N_C antennas and N^C_{RF} RF chains transmits a single stream to each IAB-node through the backhaul link [24]. If $s_m \in \mathbb{C}$ ($\mathbb{E}\{|s_m|^2\} = 1$) denotes the transmitted signal for the m-th IAB-node, the received signal at the m-th IAB-node is obtained as

$$\begin{aligned} y^{AP}_m &= \tilde{\mathbf{w}}_m\mathbf{H}^B_{m,C}\sum_{n=1}^{M}\mathbf{F}^{RF}\mathbf{f}^{BB}_n s_n + \tilde{\mathbf{w}}_m n^{AP}_m \\ &= \tilde{\mathbf{w}}_m \underbrace{\mathbf{H}^B_{m,C}\mathbf{F}^{RF}\mathbf{f}^{BB}_m s_m}_{\text{desired signal}} + \underbrace{\tilde{\mathbf{w}}_m \mathbf{H}^B_{m,C}\sum_{\substack{n=1\\ n\neq m}}^{M}\mathbf{F}^{RF}\mathbf{f}^{BB}_n s_n}_{\text{Interference}} \\ &\quad + \tilde{\mathbf{w}}_m n^{AP}_m, \end{aligned} \tag{8}$$

where $\mathbf{f}^{BB}_m$ denotes the m-th column of digital beamforming matrix $\mathbf{F}^{BB} \in \mathbb{C}^{N^C_{RF}\times M}$ and $\mathbf{F}^{RF} \in \mathbb{C}^{N_C\times N^C_{RF}}$ is the analog beamforming matrix at the IAB-donor. Also, $\tilde{\mathbf{w}}_m \in \mathbb{C}^{1\times N_A}$ is the analog beamforming vector of the m-th IAB-node in the backhaul link. Here, $n^{AP}_m \sim \mathbb{CN}(0, \sigma^2_m)$ represents the additive white Gaussian noise at each AP in the backhaul link. For fixed IAB-node locations, we only consider the LOS channel $\mathbf{H}^B_{m,C} \in \mathbb{C}^{N_A\times N_C}$ between the CPU and the m-th IAB-node that can be modeled as

$$\begin{aligned} \mathbf{H}^B_{m,C} &= \sqrt{N_C N_A}\ \zeta^L_{m,C}\ \mathbf{a}^H_L(\varphi^{AoA}_{m,C})\ \mathbf{a}_L(\varphi^{AoD}_{m,C}) \\ &\in \mathbb{C}^{N_A\times N_C}, \end{aligned} \tag{9}$$

where $\zeta^L_{m,C} \in \mathbb{CN}\left(0, 10^{-0.1\kappa}\right)$ is the path loss of the LOS channel, and $\varphi^{AoA}_{m,C}$ determines the angle of arrival.

With these assumptions, the received SINR at the m-th IAB-node in the backhaul link can be written as

$$SINR^B_m = \frac{\left|\tilde{\mathbf{w}}_m\mathbf{H}^B_{m,C}\mathbf{F}^{RF}\mathbf{f}^{BB}_m\right|^2}{\sum_{\substack{n=1\\ n\neq m}}^{M}\left|\tilde{\mathbf{w}}_m\mathbf{H}^B_{m,C}\mathbf{F}^{RF}\mathbf{f}^{BB}_n\right|^2 + \left\|\tilde{\mathbf{w}}_m\right\|^2\sigma^2_m}. \tag{10}$$

Thus, the achievable rate of the m-th IAB-node in the backhaul link can be obtained as

$$R^B_m = (1-\eta)B\log(1 + SINR^B_m). \tag{11}$$

Since in the CF systems, all APs simultaneously transmit users' signals in the access link, it is important for all APs to fully receive data streams in the backhaul link before transmitting them. Thus, the effective rate of the backhaul link becomes

$$R^B = \min_m(R^B_m). \tag{12}$$

Hence, the end-to-end network rate can be expressed as

$$R = \min(R^B, R^A). \tag{13}$$

III. PROBLEM FORMULATION

As stated before, our target in this paper is to maximize the end-to-end rate of an IAB-assisted CF massive MIMO system by optimizing the system parameters consisting of the hybrid beamforming matrices at CPU and APs and also the bandwidth allocation parameter. For maximizing the system's end-to-end rate, the minimum backhaul link rate must be greater than or equal to the access link sum rate to ensure that each IAB-node can provide the access link sum rate. Therefore, (13) equivalents to R^A, and the end-to-end rate optimization problem can be formulated as

$$\max_{\substack{\eta,\ \{\tilde{\mathbf{w}}_m\}_{m=1}^M,\ \mathbf{F}^{BB},\mathbf{F}^{RF},\\ \{\mathbf{W}^{RF}_m,\mathbf{W}^{BB}_m\}_{m=1}^M}} \quad R^A \tag{14a}$$

$$s.t.$$

$$R^B \geq R^A, \tag{14b}$$

$$\sum_{m=1}^{M}\left\|\mathbf{f}^{BB}_m\right\|^2 \leq P^B, \tag{14c}$$

$$\left|\left[\mathbf{F}^{RF}\right]_{i,j}\right|^2 = \frac{1}{N_C}\ , \forall i,j, \tag{14d}$$

$$\sum_{k=1}^{K}\left\|\mathbf{w}^{BB}_{k,m}\right\|^2 \leq P^A\ , m = 1,\ldots,M, \tag{14e}$$

$$\left|\left[\mathbf{W}^{RF}_m\right]_{i,j}\right|^2 = \frac{1}{N_A}\ , \forall i,j\ ,\ m = 1,\ldots,M, \tag{14f}$$

$$\left|\left[\tilde{\mathbf{w}}_m\right]_i\right|^2 = \frac{1}{N_A}\ , \forall i\ ,\ m = 1,\ldots,M, \tag{14g}$$

$$0 < \eta \leq 1, \tag{14h}$$

where P^B is the CPU total transmitted power constraint.

In the above optimization problem, the objective function and some constraints are non-convex due to highly coupled optimization variables and integer constraints ((14d), (14f) and (14g)). Thus, finding the optimal solution to this problem is intractable. However, by taking a close look at the problem, we observe that the backhaul and the access links have different transmitters (CPU or APs) and receivers (APs or users). Therefore, we can separately optimize each pair of the transmitters and receivers' beamforming matrices. This motivates us to propose an alternating solution to find the optimal η and then the beamforming matrices. The resulting sub-problems are presented in the following sections.

IV. MINIMUM BACKHAUL RATE MAXIMIZATION

For any given η and access link's parameters, it is evident that the performance of the access link is upper bounded with the minimum rate of the backhaul link. Therefore, in the end-to-end rate maximization problem we have to maximize the minimum backhaul link rate of APs. In this sense, (14) can be reformulated as

$$\max_{\substack{\{\tilde{\mathbf{w}}_m\}_{m=1}^M,\\ \mathbf{F}^{BB},\mathbf{F}^{RF}}} \min_m \ \log\left(1+SINR_m^B\right)$$
$$s.t.$$
$$(14c),\ (14d),\ (14g). \tag{15a}$$

By considering perfect CSI and setting $N_{RF}^C = M$, the analog beamforming matrix of the CPU can be chosen as [25]

$$\mathbf{F}^{RF} = \left[\mathbf{a}_L^H(\varphi_{1,C}^{AoD}), \mathbf{a}_L^H(\varphi_{2,C}^{AoD}), \ldots, \mathbf{a}_L^H(\varphi_{M,C}^{AoD})\right]. \tag{16}$$

In the same way, the analog beamforming vector at the m-th AP can be fixed as $\tilde{\mathbf{w}}_m = \mathbf{a}_L(\varphi_{m,C}^{AoA})$ for $m = 1, 2, \ldots, M$.

For the specified $\mathbf{F}^{RF}$ and $\{\tilde{\mathbf{w}}_m\}_{m=1}^M$, the backhaul max-min rate problem (15) can be written as

$$\max_{\mathbf{F}^{BB}} \min_m \ \log\left\{1+\frac{\left|\mathbf{b}_m\mathbf{f}_m^{BB}\right|^2}{\sum\limits_{\substack{n=1\\n\neq m}}^{M}\left|\mathbf{b}_m\mathbf{f}_n^{BB}\right|^2+\sigma_m^2}\right\}$$
$$s.t.$$
$$(14c), \tag{17a}$$

where $\mathbf{b}_m = \tilde{\mathbf{w}}_m\mathbf{H}_{m,C}^B\mathbf{F}^{RF}, m = 1, 2, \ldots, M$. By using auxiliary variable t, the above problem can be rewritten as

$$\max_{\mathbf{F}^{BB},t} \ t \tag{18a}$$
$$s.t.$$
$$\frac{\left|\mathbf{b}_m\mathbf{f}_m^{BB}\right|^2}{\sum\limits_{\substack{n=1\\n\neq m}}^{M}\left|\mathbf{b}_m\mathbf{f}_n^{BB}\right|^2+\sigma_m^2} \geq 2^t-1\ , \forall m,$$
$$(14c), \tag{18b}$$

which due to (18b), is a non-convex problem. For a fixed $t > 0$, we have the following feasibility problem.

$$Find\ \{\mathbf{F}^{BB}\} \tag{19a}$$
$$s.t.$$
$$\left(1+\frac{1}{2^t-1}\right)\left|\mathbf{b}_m\mathbf{f}_m^{BB}\right|^2 \geq \sum_{n=1}^{M}\left|\mathbf{b}_m\mathbf{f}_n^{BB}\right|^2+\sigma_m^2\ , \forall m,$$
$$(14c). \tag{19b}$$

In particular, if $t^{\circledast}$ represents the optimal value of t, we can conclude that, while the previous problem is feasible for a given t, we have $t^{\circledast} \geq t$; on the contrary, if it is infeasible, we can find that $t^{\circledast} < t$. Thus, the optimal value of t can be found by applying the bisection algorithm over t and solving some optimization problems [2]. Furthermore, when $\mathbf{F}^{BB^{\circledast}}$ is the optimal solution of (19), we can find arbitrary phase shifts $\{\phi_m\}_{m=1}^M$ for which $\mathbf{F}^{BB^{\circledast}}diag\left\{e^{j\phi_m}\right\}$ is also optimal because the absolute value of $e^{j\phi_m}$ equals 1 and it will not affect the SINR value [26]. Hence, by considering $\mathbf{b}_m\mathbf{f}_m^{BB} \geq 0$ for $\forall m$ (i.e. non-negative real valued with zero imaginary part), we can express (19b) and (14c) as the Second-order cone (SOC) constraints shown below.

$$\sqrt{1+\frac{1}{2^t-1}}\,\mathbf{b}_m\mathbf{f}_m^{BB} \geq \left\|\begin{matrix}\mathbf{b}_m\mathbf{f}_1^{BB}\\ \mathbf{b}_m\mathbf{f}_2^{BB}\\ \vdots\\ \mathbf{b}_m\mathbf{f}_M^{BB}\\ \sigma_m\end{matrix}\right\|\ , \forall m, \tag{20}$$

$$\left\|\begin{matrix}\mathbf{f}_1\\ \mathbf{f}_2\\ \vdots\\ \mathbf{f_M}\end{matrix}\right\| \leq \sqrt{P^B}. \tag{21}$$

Therefore, (19) can be reformulated as

$$Find\ \{\mathbf{F}^{BB}\}$$
$$s.t.$$
$$(20), (21), \tag{22a}$$

which is a convex second-order cone programming (SOCP) problem and can be solved by using CVX [27]. The above procedures are summarized in Algorithm 1.

V. ACCESS LINK SUM RATE MAXIMIZATION

In this section, we desire to maximize the sum rate of users in the access link by optimizing the hybrid beamforming matrix of each AP. For given η and the backhaul link's parameters, (14) can be written as

$$\max_{\{\mathbf{W}_m^{RF},\mathbf{W}_m^{BB}\}_{m=1}^M} \ R^A \tag{23a}$$
$$s.t.$$
$$\sum_{k=1}^{K}\left\|\mathbf{w}_{k,m}^{BB}\right\|^2 \leq P^A\ , m = 1, \ldots, M\ , \tag{23b}$$

Algorithm 1 Hybrid Beamforming Optimization in the Backhaul Link

Input : $\mathbf{H}^{B}_{m,C}$ for $m = 1, 2, \ldots, M$;
Initialize : $\varepsilon > 0$, $t_{\min}$, $t_{\max}$;
Compute : $\mathbf{F}^{RF}$ based on (16);
Set : $\tilde{\mathbf{w}}_m = \mathbf{a}_L(\varphi^{AoA}_{m,C})$ for $m = 1, 2, \ldots, M$;
Set : $t := \frac{t_{\min}+t_{\max}}{2}$;
Find $\{\mathbf{F}^{BB}\}$: for given t, solve (22);
if problem (22) is feasible **then**
  $t_{\min} := t$;
else
  $t_{\max} := t$;
end if;
if $t_{\max} - t_{\min} < \varepsilon$ **then**
  $\mathbf{F}^{BB} := \mathbf{F}^{BB}$;
else
  go to step (5);
end if;
Output : $\mathbf{F}^{BB}$, $\mathbf{F}^{RF}$, and $\left\{\tilde{\mathbf{w}}_m\right\}_{m=1}^{M}$.

$$\left|\left[\mathbf{W}^{RF}_{m}\right]_{i,j}\right|^2 = \frac{1}{N_A} \quad , \forall i, j \; m = 1, \ldots, M. \tag{23c}$$

Due to the non-convex objective function and integer constraints, finding the global optimal solution is intractable. Hence, we introduce a two-stage optimization strategy that optimizes the $\mathbf{W}^{RF}_{m}$ and $\mathbf{W}^{BB}_{m}$ in the different stages. As the first step, we optimize the analog beamforming matrix of each AP without considering inter-user interference. In the next step, we optimize the digital baseband beamforming matrix of each AP to eliminate interference among users in the access link. Using simulations, we demonstrate the effectiveness of our proposed decentralized hybrid beamforming, which can achieve the performance of both centralized and decentralized fully-digital beamforming.

It is mentioned that each AP is equipped with N^{A}_{RF} RF chains, where $K \leq N^{A}_{RF} \leq N_A$. Since the number of RF chains is limited, we can choose $N^{A}_{RF} = K$ and turn the main hybrid beamforming problem in (23) into computing the analog beamforming matrix and finding the corresponding baseband beamforming matrix at each AP. We assume that each user's signal is directly transmitted through one of the RF chains. Also, assuming a fully connected hybrid beamforming, each RF chain is connected to all APs' antennas with N_A phase shifters. By determining the singular value decomposition of the $\mathbf{h}_{k,m}$ as $\mathbf{h}_{k,m} = \mathbf{U}_{k,m}\sum_{k,m}\left[\mathbf{V}^{1}_{k,m}, \mathbf{V}^{0}_{k,m}\right]^{H}$, the optimal fully digital beamforming vector for the k-th user at the m-th AP will be $\mathbf{w}^{opt}_{k,m} = \mathbf{V}^{1}_{k,m} \in \mathbb{C}^{N_A \times 1}$ which is the right singular vector of the channel between the k-th user and the m-th AP. If we define $\mathbf{W}^{RF}_{m} = [\mathbf{w}^{RF}_{1,m}, \mathbf{w}^{RF}_{2,m}, \ldots, \mathbf{w}^{RF}_{K,m}]$, we can not express $\mathbf{w}^{RF}_{k,m}$ as $\mathbf{w}^{opt}_{k,m}$ for $k = 1, \ldots, K$ and $m = 1, \ldots, M$ due to the constant module constraint of the elements of the analog beamforming matrix. Thus, for maximizing the sum rate of the access link users, we minimize the distance between $\mathbf{w}^{RF}_{k,m}$ and $\mathbf{w}^{opt}_{k,m}$ [28], [29] by considering the constraints of the $\mathbf{w}^{RF}_{k,m}$ elements that can be formulated as

$$\min_{\mathbf{w}^{RF}_{k,m}} \left\|\mathbf{w}^{opt}_{k,m} - \mathbf{w}^{RF}_{k,m}\right\|^2 \tag{24a}$$

$$s.t.$$

$$\left|\left[\mathbf{w}^{RF}_{k,m}\right]_i\right|^2 = \frac{1}{N_A} \quad , i = 1, \ldots, N_A. \tag{24b}$$

We can assume $\left(\mathbf{w}^{RF}_{k,m}\right)^{H}\mathbf{w}^{RF}_{k,m} \approx \mathbf{I}_{N_A}$ since non-diagonal elements of $\left(\mathbf{w}^{RF}_{k,m}\right)^{H}\mathbf{w}^{RF}_{k,m}$ are the sum of random numbers that with high portability are lower than constant diagonal elements. Hence, by considering the orthogonal property of $\mathbf{w}^{opt}_{k,m}$, the objective function of (24) can be written as

$$\begin{aligned}\left\|\mathbf{w}^{opt}_{k,m} - \mathbf{w}^{RF}_{k,m}\right\|^2 &= Tr\left\{(\mathbf{w}^{opt}_{k,m} - \mathbf{w}^{RF}_{k,m})^{H}(\mathbf{w}^{opt}_{k,m} - \mathbf{w}^{RF}_{k,m})\right\} \\ &\propto -Tr\left\{\Re\left(\left(\mathbf{w}^{opt}_{k,m}\right)^{H}\left(\mathbf{w}^{RF}_{k,m}\right)\right)\right\}. \end{aligned} \tag{25}$$

Thus, for minimizing the objective function of (24), we can maximize

$$Tr\left\{\Re\left(\left(\mathbf{w}^{opt}_{k,m}\right)^{H}\left(\mathbf{w}^{RF}_{k,m}\right)\right)\right\} = \sum_{i=1}^{N_A}\Re\left\{\left(\left[\mathbf{w}^{opt}_{k,m}\right]_i\right)^{*}\left[\mathbf{w}^{RF}_{k,m}\right]_i\right\}. \tag{26}$$

Also, we have

$$\begin{aligned}&\Re\left\{\left(\left[\mathbf{w}^{opt}_{k,m}\right]_i\right)^{*}\left[\mathbf{w}^{RF}_{k,m}\right]_i\right\} \\ &= \left|\left[\mathbf{w}^{opt}_{k,m}\right]_i\right|\left|\left[\mathbf{w}^{RF}_{k,m}\right]_i\right|\cos\left(\angle\left[\mathbf{w}^{RF}_{k,m}\right]_i - \angle\left[\mathbf{w}^{opt}_{k,m}\right]_i\right). \end{aligned} \tag{27}$$

Obviously, for minimizing the objective function of (24), we set

$$\angle\left[\mathbf{w}^{RF}_{k,m}\right]_i = \angle\left[\mathbf{w}^{opt}_{k,m}\right]_i, \; i = 1, 2, \ldots, N_A. \tag{28}$$

To eliminate inter-user interference in the access link, we propose the Block Diagonalization (BD) algorithm that removes interference among all users by optimizing the digital beamforming matrix at each AP [30].

Based on the given analog beamforming matrix, the effective channel between the k-th user and the m-th AP in the access link can be expressed as

$$\bar{\mathbf{h}}_{k,m} = \mathbf{h}_{k,m}\,\mathbf{W}^{RF}_{m} \in \mathbb{C}^{1\times N^{A}_{RF}}. \tag{29}$$

Thus, for inter-user interference cancellation, based on the given $\bar{\mathbf{h}}_{k,m}$, the baseband digital precoder of each user should be orthogonal to the effective channel of other users (i.e. $\bar{\mathbf{h}}_{j,m}\,\mathbf{w}^{BB}_{k,m} = 0 \; ; k \neq j$ where $\mathbf{w}^{BB}_{k,m}$ indicates the k-th column of $\mathbf{W}^{BB}_{m}$). To be more specific, if we define $\tilde{\mathbf{H}}_{k,m} = \left[\bar{\mathbf{h}}^{T}_{1,m}|\bar{\mathbf{h}}^{T}_{2,m}|\ldots|\bar{\mathbf{h}}^{T}_{k-1,m}|\bar{\mathbf{h}}^{T}_{k+1,m}|\ldots|\bar{\mathbf{h}}^{T}_{K,m}\right]^{T} \in \mathbb{C}^{K-1\times N^{A}_{RF}}$, the $\mathbf{w}^{BB}_{k,m}$ should be laid in the null space of $\tilde{\mathbf{H}}_{k,m}$. In this regard, by introducing $r = rank(\tilde{\mathbf{H}}_{k,m})$, which has to satisfy

$r_{k,m} \leq K-1$, the singular value decomposition (SVD) of $\tilde{\mathbf{H}}_{k,m}$ can be written as

$$\begin{aligned}\tilde{\mathbf{H}}_{k,m} &= \tilde{\mathbf{U}}_{k,m}\tilde{\Sigma}_{k,m}\tilde{\mathbf{V}}^{H}_{k,m} \\ &= \tilde{\mathbf{U}}_{k,m}\tilde{\Sigma}_{k,m}\left[\tilde{\mathbf{V}}^{1}_{k,m}\ \tilde{\mathbf{V}}^{0}_{k,m}\right]^{H},\end{aligned} \tag{30}$$

where $\tilde{\mathbf{V}}^{1}_{k,m}$ and $\tilde{\mathbf{V}}^{0}_{k,m}$ represent $\tilde{\mathbf{V}}_{k,m}(:, 1 : r_{k,m})$ and $\tilde{\mathbf{V}}_{k,m}(:, r_{k,m}+1 : end)$, respectively. It is clear that $\tilde{\mathbf{V}}^{0}_{k,m}$ includes the orthogonal basis of the null space of $\tilde{\mathbf{H}}_{k,m}$, so $\bar{\mathbf{h}}_{j,m}\tilde{\mathbf{V}}^{0}_{k,m}$ can be formulated as

$$\bar{\mathbf{h}}_{j,m}\tilde{\mathbf{V}}^{0}_{k,m} = \begin{cases} 0\,;\ k \neq j \\ \mathbf{U}_{k,m}\Sigma_{k,m}\mathbf{V}^{H}_{k,m}\,;\ k = j \end{cases}. \tag{31}$$

Let us define $\mathbf{V}_{k,m}$ as $\mathbf{V}_{k,m}=\left[\mathbf{V}^{1}_{k,m}\ \mathbf{V}^{0}_{k,m}\right]$, where $\mathbf{V}^{1}_{k,m}$ is the first column of $\mathbf{V}^{H}_{k,m}$. As a result, for jointly suppressing the inter-user interference and enhancing the spectrum efficiency, the digital beamforming matrix of the m-th AP can be expressed as

$$\mathbf{W}^{BB}_{m} = \left[\tilde{\mathbf{V}}^{0}_{1,m}\,\mathbf{V}^{1}_{1,m}, \tilde{\mathbf{V}}^{0}_{2,m}\,\mathbf{V}^{1}_{2,m}, \ldots, \tilde{\mathbf{V}}^{0}_{K,m}\,\mathbf{V}^{1}_{K,m}\right]. \tag{32}$$

The above procedure is summarized in Algorithm 2, where $(*)$ is defined to satisfy the APs power constraints in the access link [31].

Algorithm 2 Optimal Hybrid Beamforming Design in the Access Link

Input : $\mathbf{h}_{k,m}$ for $\forall k, m$;
RepeatforeachAP :
Compute : $\mathbf{W}^{RF}_{m}$ based on (28);
Compute :
for $k = 1$ **to** K **do**
  $\bar{\mathbf{h}}_{k,m} = \mathbf{h}_{k,m}\,\mathbf{W}^{RF}_{m}$;
  $\tilde{\mathbf{H}}_{k,m} = \left[\bar{\mathbf{h}}^{T}_{1,m}|\bar{\mathbf{h}}^{T}_{2,m}|\ldots|\bar{\mathbf{h}}^{T}_{k-1,m}|\bar{\mathbf{h}}^{T}_{k+1,m}|\ldots|\bar{\mathbf{h}}^{T}_{K,m}\right]^{T}$;
  $\tilde{\mathbf{H}}_{k,m} = \tilde{\mathbf{U}}_{k,m}\tilde{\Sigma}_{k,m}\left[\tilde{\mathbf{V}}^{1}_{k,m}\ \tilde{\mathbf{V}}^{0}_{k,m}\right]^{H}$;
  $\bar{\mathbf{h}}_{k,m}\,\tilde{\mathbf{V}}^{0}_{k,m} = \mathbf{U}_{k,m}\Sigma_{k,m}\mathbf{V}^{H}_{k,m}$;
  $\mathbf{W}^{BB}_{m} = \left[\tilde{\mathbf{V}}^{0}_{1,m}\,\mathbf{V}^{1}_{1,m}, \tilde{\mathbf{V}}^{0}_{2,m}\,\mathbf{V}^{1}_{2,m}, \ldots, \tilde{\mathbf{V}}^{0}_{K,m}\,\mathbf{V}^{1}_{K,m}\right]$;
  $\mathbf{W}^{BB}_{m} = \frac{P^{A}\,\mathbf{W}^{BB}_{m}}{\|\mathbf{W}^{BB}_{m}\|_{F}}$ $(*)$;
end for;
Output : $\{\mathbf{W}^{BB}_{m}, \mathbf{W}^{RF}_{m}\}_{m=1}^{M}$.

VI. BANDWIDTH ALLOCATION COEFFICIENT OPTIMIZATION

In the previous sections, the minimum backhaul rate and access link sum-rate have been maximized (in bps/Hz). Now we try to find an optimal bandwidth allocation coefficient that satisfies (14)'s constraints and maximize its objective function. Hence, (14) can be rewritten as

$$\max_{\eta} \quad \eta\, C_A \tag{33a}$$
$$s.t. \quad (1-\eta)\, C_B \geq \eta\ C_A, \tag{33b}$$
$$0 < \eta \leq 1, \tag{33c}$$

where C_A and C_B are given as

$$C_A = B\sum_{k=1}^{K}\log\left(1+\frac{\sum_{m=1}^{M}\left|\mathbf{h}_{k,m}\mathbf{W}^{RF}_{m}\mathbf{w}^{BB}_{k,m}\right|^{2}}{\sum_{\substack{j=1\\ j\neq k}}^{K}\sum_{m=1}^{M}\left|\mathbf{h}_{k,m}\mathbf{W}^{RF}_{m}\mathbf{w}^{BB}_{j,m}\right|^{2}+\sigma^{2}_{k}}\right), \tag{34}$$

$$C_B = \min_{m}\ B\log\left(1+\frac{\left|\tilde{\mathbf{w}}_{m}\mathbf{H}^{B}_{m,C}\,\mathbf{F}^{RF}\,\mathbf{f}^{BB}_{m}\right|^{2}}{\sum_{\substack{n=1\\ n\neq m}}^{M}\left|\tilde{\mathbf{w}}_{m}\mathbf{H}^{B}_{m,C}\,\mathbf{F}^{RF}\,\mathbf{f}^{BB}_{n}\right|^{2}+\sigma^{2}_{m}}\right). \tag{35}$$

If we rewrite (33b) as $\eta \leq \frac{C_B}{C_A+C_B}$, it is clear that η is upper bounded, so the maximum value of η (i.e. optimal value of (33)) can be found as

$$\eta = \frac{C_B}{C_A + C_B}. \tag{36}$$

Therefore, based on (36) and (34) (or 35), the end-to-end rate of the proposed system determined in (13) can be calculated as

$$R = \frac{C_A\, C_B}{C_A + C_B}. \tag{37}$$

In the above sections, we optimize all optimization parameters. Algorithm 3 summarizes the CF massive MIMO system end-to-end rate optimization. Using this algorithm, the hybrid beamforming matrices of the access and backhaul links can be optimized simultaneously. The bandwidth allocation coefficient is then calculated using the C_A and C_B parameters. It should be noted that the proposed hybrid beamforming algorithm in the access link is locally calculated by each AP. Then, each user's desired and interference signals should be sent to the CPU by each AP. In the following, we evaluate the access link performance for decentralized beamforming at each AP and centralized beamforming at the CPU and evaluate the backhaul resources required for each scenario.

Algorithm 3 End-to-End Rate Optimization in the CF Massive MIMO Systems

Input : $\mathbf{h}_{k,m}$, $\mathbf{H}^{B}_{m,C}$; $\forall k, m$;
Optimize: the backhaul link parameters via Algorithm 1 and optimize the access link parameters via Algorithm 2;
Find: optimum bandwidth allocation coefficient based on the (36).

TABLE 1. CF massive MIMO system parameters.

PARAMETER	NOTATION	VALUE
LOS link path loss exponent	α	2.1 [32]
NLOS link path loss exponent	α	3.64 [32]
Number of the users	K	8
Number of the CPU's antenna	N_C	64
AP's antennas for Access	N_A	64 [33]
Number of NLOS path	$L_{k,m}$	5
Career frequency	f_c	28 GHz
System bandwidth	B	2 GHz [12]
Noise variance in Access	σ_k^2	-174 dBm/Hz [12]
Noise variance in Backhaul	σ_m^2	-174 dBm/Hz [12]
AP-CPU distance	$d_{A-C}(m)$	$30 \leq d_{A-C} \leq 50$
User-AP distance	$d_{U-A}(m)$	$150 \leq d_{U-A} \leq 200$

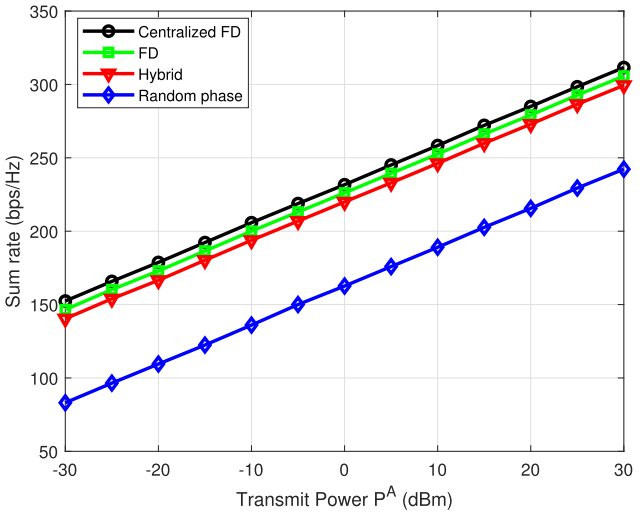

FIGURE 2. Sum rate of Access link users versus different transmitter power constraint with $M = 6, K = 8$.

TABLE 2. Backhaul link resources for the access link beamforming optimization.

Beamforming	UL	DL
Centralized-FD	MN_AK	$1 + MN_AK$
Decentralized-FD	$2MK$	1
Decentralized-Hybrid	$2MK$	1

VII. SIMULATION RESULTS

In this section, we evaluate performance of the proposed scheme by computer simulation. The performance of the backhaul and access links are evaluated based on the number of IAB-nodes, transmit power constraints, and different bandwidth allocation coefficients. The simulation parameters are shown in Table 1.

First, we compare our proposed hybrid beamforming BD-based algorithm with the fully digital (shown by FD abbreviation) BD algorithm [30] (i.e., when the number of RF chains equals to the number of the transmitter's antennas) and random analog beamforming matrices. Fig. 2 illustrates the sum rate of users (in bps/Hz) in the access link versus the AP's transmitter power constraints. It can be seen that our proposed hybrid BD algorithm approximately achieves the same performance as fully-digital BD. Also, it significantly outperforms random beamforming. This figure also

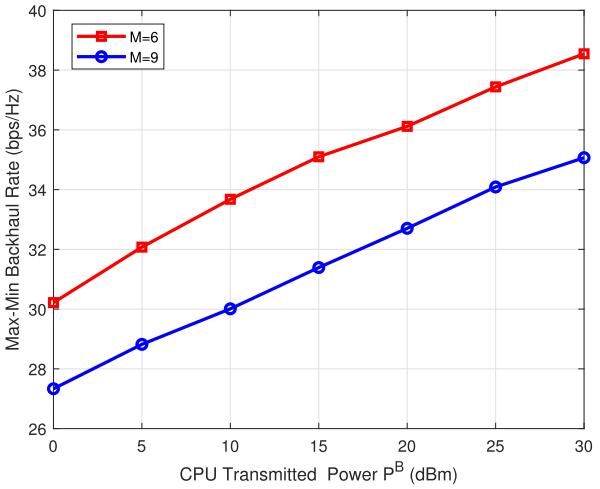

FIGURE 3. Max-Min rate of APs in the Backhaul link versus different power constraints and number of APs.

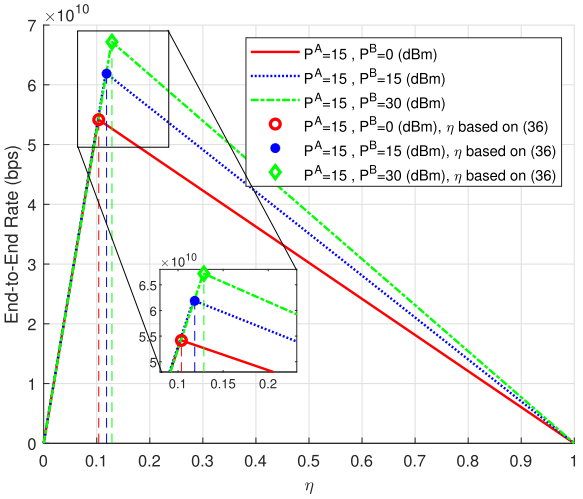

FIGURE 4. End-to-end rate versus different values of η with $M = 6, K = 8$.

presents the performance of the centralized FD beamforming algorithm, in which the CPU designs the beamforming matrix of each AP in the access link using the CSI of all users. It is observed that a centralized beamforming can increase the access link rate of the users, but the instantaneous CSI of each user must be provided for the CPU. Backhaul resources that should be used in the centralized and decentralized scenarios are shown in Table 2. In the centralized fully-digital system, each AP has to transmit its channel to all users in the UL to receive the optimal fully-digital beamforming matrix and bandwidth allocation parameter in the DL. However, in the decentralized systems, each AP sends each user's desired and interference signals, which are used in (34), and the CPU should only send back the bandwidth allocation parameter in the DL. We can see in Table 2 that the centralized beamforming optimization requires considerable backhaul resources, especially in large antenna cases, but does not provide a significant improvement.

Fig. 3 shows how increasing the number of IAB-nodes will reduce the max-min rate of the IAB-nodes in the backhaul

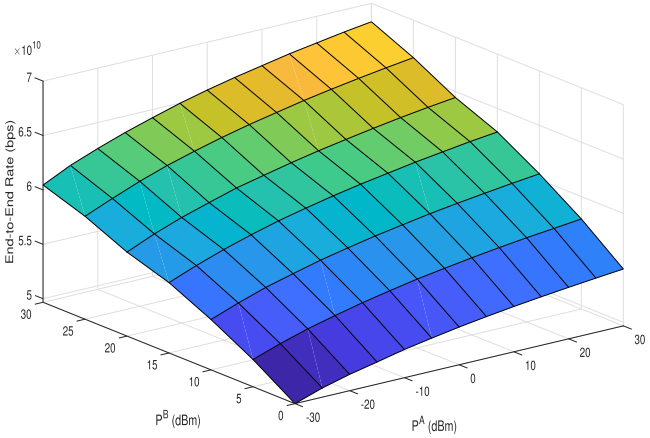

FIGURE 5. End-to-end rate versus the access and backhaul links power constraints with $M = 6, K = 8$.

link due to the inter-IAB-node interference. In fact, increasing the number of IAB-nodes can inversely affect the max-min rate of the IAB-nodes in the backhaul link and directly affect the sum rate of the access link's users.

Fig. 4 depicts the end-to-end rate of the system using an exhaustive search through all possible η values. The end-to-end rate is also determined based on the bandwidth allocation coefficient that has been defined in (36). It can be seen that the proposed bandwidth allocation strategy maximizes the end-to-end rate of the system for different power constraints in the access and backhaul links. According to the figure, improving one link will result in more bandwidth being allocated to another. For example, by increasing the backhaul link power constraint from 0 dBm to 30 dBm, the system has to allocate more bandwidth to the access link to maximize the end-to-end rate.

Fig. 5 shows the end-to-end rate of the system versus the access and backhaul links power constraints. It can be observed that by decreasing the access link APs power, the end-to-end rate is less affected by backhaul link power constraints, indicating that the access link limits the system's performance. In the same way, the end-to-end rate is affected slowly by the access link power variation as the backhaul link power decreases. As a result, we can conclude that we need to provide enough power for both the access and backhaul links to achieve a specified end-to-end data rate.

In Fig. 6, we evaluate coverage without taking into consideration the NLOS paths in (2). This figure shows the end-to-end rate of the network for different numbers of APs. Based on (13), the end-to-end rate of the network corresponds to the minimum rate of the access and backhaul links. When there are only a small number of APs, the end-to-end rate of the network is the same as the data rate of the access link. As the data rate of the access link increases, the end-to-end rate of the network also increases. But if the number of APs grows, the end-to-end rate of the network is determined by the data rate of the backhaul link and decreases as the backhaul link's rate decreases. This shows that an optimum number of APs can be found in the system, which is 9 in this setting.

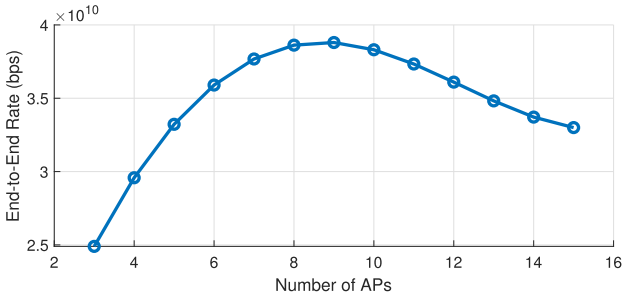

FIGURE 6. End-to-end rate versus the different number of APs with $P^A = 30$ dBm, $P^B = 30$ dBm.

VIII. CONCLUSION

In this paper, we considered a CF massive MIMO system and maximized the end-to-end rate of the users by optimizing the hybrid beamforming matrices of the CPU and the IAB-nodes in the backhaul and access links, respectively. For integrating the two link types, we developed a close-form expression for the bandwidth allocation coefficient between the access and backhaul links. In comparison to fully digital beamforming, the simulation results demonstrate the effectiveness of the proposed hybrid beamforming algorithm. Furthermore, for different power constraints in the access and backhaul links, the proposed bandwidth allocation strategy maximizes the end-to-end rate of the system. The end-to-end rate of the system was analyzed by an increasing number of IAB-nodes, demonstrating that the end-to-end rate of the users first increased and then decreased due to the access and backhaul links' limitations. Therefore, due to the dependence of the end-to-end rate of the users in both access and backhaul links, increasing the number of IAB-nodes in these systems may not always be beneficial.

REFERENCES

[1] E. Björnson, J. Hoydis, and L. Sanguinetti, "Massive MIMO networks: Spectral, energy, and hardware efficiency," *Found. Trends Signal Process.*, vol. 11, nos. 3–4, pp. 154–655, 2017.

[2] H. Q. Ngo, A. Ashikhmin, H. Yang, E. G. Larsson, and T. L. Marzetta, "Cell-free massive MIMO versus small cells," *IEEE Trans. Wireless Commun.*, vol. 16, no. 3, pp. 1834–1850, Mar. 2017.

[3] H. Q. Ngo, A. Ashikhmin, H. Yang, E. G. Larsson, and T. L. Marzetta, "Cell-free massive MIMO: Uniformly great service for everyone," in *Proc. IEEE 16th Int. Workshop Signal Process. Adv. Wireless Commun. (SPAWC)*, Jun. 2015, pp. 201–205.

[4] U. K. Ganesan, E. Björnson, and E. G. Larsson, "An algorithm for grant-free random access in cell-free massive MIMO," in *Proc. IEEE 21st Int. Workshop Signal Process. Adv. Wireless Commun. (SPAWC)*, May 2020, pp. 1–5.

[5] J. Kassam, D. Castanheira, A. Silva, R. Dinis, and A. Gameiro, "Distributed hybrid equalization for cooperative millimeter-wave cell-free massive MIMO," *IEEE Trans. Commun.*, vol. 70, no. 8, pp. 5300–5316, Aug. 2022.

[6] S. Buzzi, C. D'Andrea, A. Zappone, and C. D'Elia, "User-centric 5G cellular networks: Resource allocation and comparison with the cell-free massive MIMO approach," *IEEE Trans. Wireless Commun.*, vol. 19, no. 2, pp. 1250–1264, Feb. 2020.

[7] H. A. Ammar, R. Adve, S. Shahbazpanahi, G. Boudreau, and K. V. Srinivas, "User-centric cell-free massive MIMO networks: A survey of opportunities, challenges and solutions," 2021, *arXiv:2104.14589*.

[8] B. Tezergil and E. Onur, "Wireless backhaul in 5G and beyond: Issues, challenges and opportunities," 2021, *arXiv:2103.08234*.

[9] C. Madapatha, B. Makki, C. Fang, O. Teyeb, E. Dahlman, M. Alouini, and T. Svensson, "On integrated access and backhaul networks: Current status and potentials," *IEEE Open J. Commun. Soc.*, vol. 1, pp. 1374–1389, 2020.

[10] *Nr; Study on Integrated Access and Backhaul; Release 15*, document TR 38.874, 3GPP, 2018.

[11] S. Hur, T. Kim, D. J. Love, J. V. Krogmeier, T. A. Thomas, and A. Ghosh, "Millimeter wave beamforming for wireless backhaul and access in small cell networks," *IEEE Trans. Commun.*, vol. 61, no. 10, pp. 4391–4403, Oct. 2013.

[12] S. Ni, J. Zhao, H. H. Yang, and Y. Gong, "Enhancing downlink transmission in MIMO HetNet with wireless backhaul," *IEEE Trans. Veh. Technol.*, vol. 68, no. 7, pp. 6817–6832, Jul. 2019.

[13] M. Polese, M. Giordani, A. Roy, S. Goyal, D. Castor, and M. Zorzi, "End-to-end simulation of integrated access and backhaul at mmWaves," in *Proc. IEEE 23rd Int. Workshop Comput. Aided Model. Design Commun. Links Netw. (CAMAD)*, Sep. 2018, pp. 1–7.

[14] J. Y. Lai, W. Wu, and Y. T. Su, "Resource allocation and node placement in multi-hop heterogeneous integrated-access-and-backhaul networks," *IEEE Access*, vol. 8, pp. 122937–122958, 2020.

[15] C. Madapatha, B. Makki, A. Muhammad, E. Dahlman, M.-S. Alouini, and T. Svensson, "On topology optimization and routing in integrated access and backhaul networks: A genetic algorithm-based approach," 2021, *arXiv:2102.07252*.

[16] C. Fang, C. Madapatha, B. Makki, and T. Svensson, "Joint scheduling and throughput maximization in self-backhauled millimeter wave cellular networks," in *Proc. 17th Int. Symp. Wireless Commun. Syst. (ISWCS)*, 2021, pp. 1–6.

[17] H. Q. Ngo, L. Tran, T. Q. Duong, M. Matthaiou, and E. G. Larsson, "On the total energy efficiency of cell-free massive MIMO," *IEEE Trans. Green Commun. Netw.*, vol. 2, no. 1, pp. 25–39, Mar. 2018.

[18] Q. N. Le, V. Nguyen, O. A. Dobre, and R. Zhao, "Energy efficiency maximization in RIS-aided cell-free network with limited backhaul," *IEEE Commun. Lett.*, vol. 25, no. 6, pp. 1974–1978, Jun. 2021.

[19] U. Demirhan and A. Alkhateeb, "Enabling cell-free massive MIMO systems with wireless millimeter wave fronthaul," 2021, *arXiv:2110.01798*.

[20] M. R. Akdeniz, Y. Liu, M. K. Samimi, S. Sun, S. Rangan, T. S. Rappaport, and E. Erkip, "Millimeter wave channel modeling and cellular capacity evaluation," *IEEE J. Sel. Areas Commun.*, vol. 32, no. 6, pp. 1164–1179, Jun. 2014.

[21] P. Wang, J. Fang, X. Yuan, Z. Chen, and H. Li, "Intelligent reflecting surface-assisted millimeter wave communications: Joint active and passive precoding design," *IEEE Trans. Veh. Technol.*, vol. 69, no. 12, pp. 14960–14973, Dec. 2020.

[22] K. Haneda, "5G 3GPP-like channel models for outdoor urban microcellular and macrocellular environments," in *Proc. IEEE 83rd Veh. Technol. Conf. (VTC-Spring)*, May 2016, pp. 1–7.

[23] G. R. MacCartney and T. S. Rappaport, "Study on 3GPP rural macrocell path loss models for millimeter wave wireless communications," in *Proc. IEEE Int. Conf. Commun. (ICC)*, May 2017, pp. 1–7.

[24] G. Kwon and H. Park, "Joint user association and beamforming design for millimeter wave UDN with wireless backhaul," *IEEE J. Sel. Areas Commun.*, vol. 37, no. 12, pp. 2653–2668, Dec. 2019.

[25] B. Ning, Z. Chen, W. Chen, Y. Du, and J. Fang, "Terahertz multi-user massive MIMO with intelligent reflecting surface: Beam training and hybrid beamforming," *IEEE Trans. Veh. Technol.*, vol. 70, no. 2, pp. 1376–1393, Feb. 2021.

[26] A. Wiesel, Y. C. Eldar, and S. Shamai Shitz, "Linear precoding via conic optimization for fixed MIMO receivers," *IEEE Trans. Signal Process.*, vol. 54, no. 1, pp. 161–176, Jan. 2006.

[27] M. Grant and S. Boyd. (Mar. 2014). *CVX: MATLAB Software for Disciplined Convex Programming Version 2.1*. [Online]. Available: http://cvxr.com/cvx

[28] X. Yu, J. Shen, J. Zhang, and K. B. Letaief, "Alternating minimization algorithms for hybrid precoding in millimeter wave MIMO systems," *IEEE J. Sel. Topics Signal Process.*, vol. 10, no. 3, pp. 485–500, Apr. 2016.

[29] O. E. Ayach, R. W. Heath, S. Abu-Surra, S. Rajagopal, and Z. Pi, "Low complexity precoding for large millimeter wave MIMO systems," in *Proc. IEEE Int. Conf. Commun. (ICC)*, Jun. 2012, pp. 3724–3729.

[30] Q. H. Spencer, A. L. Swindlehurst, and M. Haardt, "Zero-forcing methods for downlink spatial multiplexing in multiuser MIMO channels," *IEEE Trans. Signal Process.*, vol. 52, no. 2, pp. 461–471, Feb. 2004.

[31] O. E. Ayach, S. Rajagopal, S. Abu-Surra, Z. Pi, and R. W. Heath, "Spatially sparse precoding in millimeter wave MIMO systems," *IEEE Trans. Wireless Commun.*, vol. 13, no. 3, pp. 1499–1513, Mar. 2014.

[32] J. Lee, J. Choi, J. Lee, and S. Kim, "28 GHz millimeter-wave channel models in urban microcell environment using three-dimensional ray tracing," *IEEE Antennas Wireless Propag. Lett.*, vol. 17, no. 3, pp. 426–429, Mar. 2018.

[33] Y. Jin, J. Zhang, S. Jin, and B. Ai, "Channel estimation for cell-free mmWave massive MIMO through deep learning," *IEEE Trans. Veh. Technol.*, vol. 68, no. 10, pp. 10325–10329, Oct. 2019.

ALI HOSSEINALIPOUR JAZI received the B.Sc. degree in electrical communication engineering from the University of Kashan, Kashan, Iran, in 2019, and the M.Sc. degree in communication system engineering from the Iran University of Science and Technology (IUST), Tehran, Iran, in 2022. He is currently a researcher in the field of communication systems engineering. His research interests include wireless communication and signal processing techniques, especially integrated access and backhaul (IAB), hybrid beamforming techniques, and intelligent reflecting surfaces (IRSs).

S. MOHAMMAD RAZAVIZADEH (Senior Member, IEEE) received the B.Sc., M.Sc., and Ph.D. degrees in electrical engineering from the Iran University of Science and Technology (IUST), in 1997, 2000, and 2006, respectively. He is currently an Associate Professor with the School of Electrical Engineering in IUST and also serves as the Head of the Iran Telecommunications Research Center (ITRC). Prior to joining IUST in 2011, he worked as a Research Assistant Professor at ITRC, from 2006 to 2011. Throughout his career, he has held visiting positions at the University of Waterloo, Korea University, and Chalmers University of Technology. His research primarily focuses on wireless communication systems and signal processing within these networks.

TOMMY SVENSSON (Senior Member, IEEE) received the Ph.D. degree in information theory from Chalmers, in 2003. He is currently a Full Professor of communication systems with the Chalmers University of Technology, Gothenburg, Sweden, where he is leading the wireless systems research on air interface and wireless backhaul networking technologies for future wireless systems. He was with Ericsson AB in core networks, radio access networks, and microwave transmission products. He was involved in the European WINNER and ARTIST4G Projects, which made important contributions to the 3GPP LTE Standards, the EU FP7 METIS, and the EU H2020 5GPPP mmMAGIC and 5GCar projects toward 5G; and currently the Hexa-X, RISE-6G, and SEMANTIC projects toward 6G. He was in the ChaseOn antenna systems excellence center at Chalmers targeting mm-wave and (sub)-THz solutions for 5G/6G access, backhaul/fronthaul, and V2X scenarios. He has coauthored five books. His research interests include design and analysis of physical layer algorithms, multiple access, resource allocation, cooperative systems, moving networks, and satellite networks. He served as a Coordinator for the Communication Engineering Master's Program at Chalmers.